Analysis of a Large-Scale Landslide Using Shear Strength Reduction Factor Method, Case Study: Manjil Landslide

Mahnaz Firuzi[*1], Mohammad H. Ghobadi[1], Ali Noorzad[2], Ehsan Dadashi[3]

1. Department of Geology, Bu-Ali Sina University, Hamadan, IRAN
2. Faculty of Civil, Water and Environmental Engineering, Shahid Beheshti University, Tehran, IRAN
3. Ph.D of Rock Mechanic, Tehran, IRAN

Received: 3 April 2017 Revised: 17 Oct 2017

Abstract

Slope stability could be a major concern during the construction of infrastructures. This study is focused to analyze the slope stability of Manjil landslide that was located 41+400 to 42+200 km along Qazvin-Rasht freeway, Iran. The Manjil landslide, which had 168 m long and approximately 214 m wide, was occurred due to inappropriate cutting in June 2013 and led to destructive and closure of freeway. Slope stability analysis was carried out using a finite element shear strength reduction method (FE-SRM). The PHASE^{2D} program was utilized in order to model the slope cutting and stability of landslide. Slope angle was flatted with 3H:2V geometry and stabilized with piling. The results indicated safety factors of 1.95 and 1.17 in the static and pseudo-static states, respectively, while the maximum bending moment with single pile (SP) in the pseudo-static

[*]Corresponding author Firuzi.mahnaz@yahoo.com

[Downloaded from ndea10.khu.ac.ir on 2026-11-03]

[DOR: 20.1001.1.22286837.1398.13.5.4.3]

state was 5.69 MN. Maximum bending moment of the pile around the slip surface was significantly large and more than the bending moment capacity of the pile. Due to the large bending moment on the pile, pile-to-pile cap connections (two pile group: 2PG) should be designed at the toe of the slope. The obtained results showed reduction of this parameter to 2.48 MN. Thus, it can be concluded that 2PG is a suitable stabilization method for the Manjil landslide.

Keywords: Manjil landslide, Finite element model, Shear strength reduction factor method, Pile-to-pile cap connections, Stability analysis.

[Downloaded from ndea10.khu.ac.ir on 2026-11-03]

[DOR: 20.1001.1.22286837.1398.13.5.4.3]

Introduction

Slope stabilization requires focusing on the selection of appropriate and cost-effective landslide remedial measurements. In particular, when slope instability processes affect directly or indirectly the roads or railways, the economic consequences of heavy traffic for even a short period of time can far outweigh the remedial costs [1]. In order to evaluate slope stability, various methods have been proposed using the limit equilibrium analysis [2, 3, 4, 5 and 6]. Geotechnical engineers usually use this method to analyze the stability and design the embankments and excavations. Although this method is very simple, it involves some disadvantages; first, the stress-strain behavior of the soil or rock mass is not taken into account in calculation of the factor of safety. Second, the shape of critical slip surface must be searched with trial and error. The failure initiation point and its development are unknown; finally, the initial stresses are not considered in the limit equilibrium analysis [7]. Many researchers applied different numerical techniques for

continuum and dis-continuum media to solve the problems related to limit equilibrium methods. The finite element method (FEM) represent one of the powerful alternative approaches for slope stability analysis due to its accuracy and versatility, as well as few assumptions [8]. Moreover, finite element analysis with shear strength reduction (SSR), which is based on the Mohr-Coulomb failure criterion and considers the reduction of cohesion and friction angle, replaces the conventional limit equilibrium. Budetta (2011) [9], Usluogullari et al. (2016) [10] and Chen et al. (2016) [11] performed SSR for slope stability analysis.

A number of slope stabilization approaches are introduced to prevent potential hazards such as benching, piles, retaining walls, anchors, soil nailing and drainage systems [10]. Piles have been successfully used in many situations to stabilize slopes or to improve slope stability. In this regard, numerous methods have been developed for the analysis of piled slopes. Several studies have been conducted to evaluate the efficiency of pile location from top to the toe of the slip surface [12]. Ashour and Ardalan (2012) [13] indicated that for slopes with two layers of soil where a soft layer is overlying on stiff layer, piles should be installed between middle and top of the slip surface. The numerical analysis was carried out using a finite element method (FEM) formulation with SSR method in Mohr-Coulomb model provided in the PHASE^{2D} [14].

The aim of this paper is the study of Manjil landslide located at 41+400 km to 42+200 km along the Qazvin-Rasht freeway, Iran. Two methods are proposed to improve the slope stability; soil

[Downloaded from ndea10.khu.ac.ir on 2026-11-03]

[DOR: 20.1001.1.22286837.1398.13.5.4.3]

removing and using single pile (SP) besides soil removing and using pile-to-pile cap connections (two pile group: 2PG**)**. In order to determine an optimal method, a factor of safety (FS), the maximum bending moment, the maximum shear force and the maximum shear displacement of the structural elements in the static and pseudo-static states are computed. Hence, in this research, a comprehensive comparison of two slope stabilization methods is presented to give an insight into selecting the proper stabilization method and understanding the behavior of supporting systems.

Study area

Manjil landslide is situated at the Qazvin-Rasht freeway (41+400 km to 42+200 km) in the northern Manjil city, within the coordinate 49˚ 24' 1.13" E and 36˚ 45' 1.98" N to 49˚ 24' 7.23" E and 36˚ 45' 0.07" N at an elevation of about 2,000 m. This landslide is situated on the northwest-southeast facing slope on the right side of Sefid Rud dam. The location of the landslide area, freeway and its surroundings on the shaded-relief map are displayed in Figure 1.

Deformation characteristics

Slope cutting in the toe to construct Qazvin-Rasht freeway was started in June 2013. The berms were designed with a width and height of 4 m and 6 m, respectively, and a 5-6 m excavation depth at 120 m intervals in the slope's toe (Figure 2). During the excavation, large fissures began to appear at the cutting edge excavation phase. Subsequently, on July 2013, the road was progressively appeared

[Downloaded from ndea10.khu.ac.ir on 2026-11-03]

[DOR: 20.1001.1.22286837.1398.13.5.4.3]

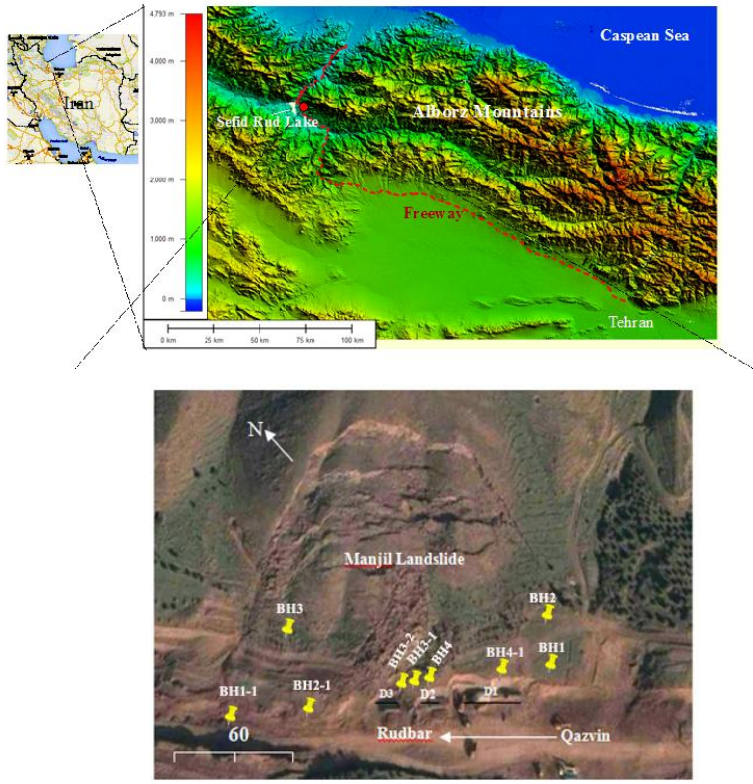


Figure 1. Location of the landslide area, freeway, and its surroundings on the shaded-relief map and google earth image of Manjil landslide acquired on 6 August 2013. The boreholes drilled in the front the toe slope are depicted in the figure.

with mass movement and debris and led blockage of the freeway.

The slope height, width and angle were approximately 25, 168 m, and 45˚, respectively. The overall slope angle before the landslide occurrence was 22˚. It is clear that cutting with these characteristics reduces the shear strength of material leading to the slip occurrence. After the first failure, it was planned to construct three retaining walls in front of cutting slope in order to stabilize Manjil landslide.

[Downloaded from ndea10.khu.ac.ir on 2026-11-03]

[DOR: 20.1001.1.22286837.1398.13.5.4.3]

Despite the construction of the retaining wall, displacements were observed due to the re-failure of the slope on the existing slip surface. Thus, the slope was still unstable. After the failure, it was planned to construct three retaining walls (D_1, D_2, and D_3) to stabilize the landslide. But due to lack of sustainable design were not stable. Walls D_1 and D_2 were 10 m (L) while D_3 was 30 m long. In Figure. 2, the three walls and concrete blocks are shown.

The landslide was approximately 168 m long and 214 m wide, with a total of area of about 470,000 m^3. The scarp was located at an elevation of 375 m, approximately 40 m above the toe. The sliding direction of the landslide was 240˚ approximately perpendicular to the freeway (130˚). Manjil landslide and its components are illustrated in Figure 3. As seen in the figure, this landslide is a complex, displaying composite rotational-debris flow. Can (2014) [15] reported that the rotational slides are encountered mostly by geotechnical engineers along the roads and highways. In this landslide, the surface rupture to the curve is upward and concave and



Figure 2. A view of the cutting slope with four berms of 4 m width and 6 m height (1H: 2V) and heavy works during the 5-6 m excavation on the toe of slope along 41+400 to 42+200 km of Qazvin-Rasht freeway

[Downloaded from ndea10.khu.ac.ir on 2026-11-03]

[DOR: 20.1001.1.22286837.1398.13.5.4.3]

the slide movement is approximately rotational about an axis parallel to the ground surface and transverse across the slide. Moreover, the surface of rupture begins with the main scarp slope of 75˚. The following type of landslide is formed by a combination of loose alluvial sedimentary (Q^{al}), red color marls and tuffs reaching the other side of the road and covering the entire width of the freeway.

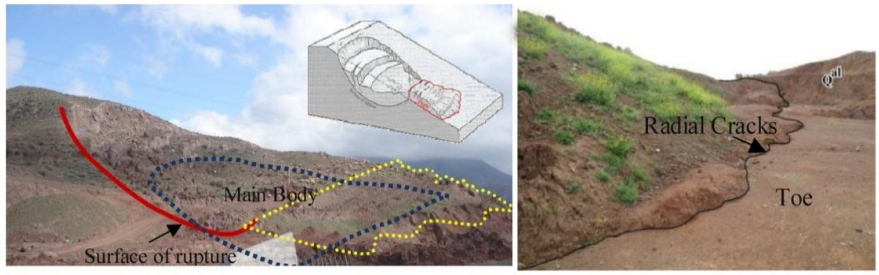


Figure 3. Manil landslide formation and its components

Geological setting

The main geological unit outcropped in the landslide area is Karaj formation, which is a well-known formation of the Alborz mountains. This formation is composed of a variety of pyroclastic rocks, often interbedded with sedimentary rocks. The characteristic rock type is tuff breccias, and sandy and silty tuffs occur together with shales, siltstones and sandstones. Other units which appeared during the cutting (Figure 4a, 4b, and 4c) have also important roles in the preparation of geological section. The geological map of the Manjil landslide and its geological section are presented in Figures 5 and 6, respectively. Quaternary alluvial river deposits (Q^{al}) are composed of clay and fragment grains mainly distributed in the mountain front and lie unconformably on the Eocene sandstones, red colored marls, and sometimes shale with layers of clay (Figure 4a).

[Downloaded from ndea10.khu.ac.ir on 2026-11-03]

[DOR: 20.1001.1.22286837.1398.13.5.4.3]



Figure 4. a) A view of the Q_t at Manjil landslide lie discontinuously on the volcanic breccias (VB) as well as VB lie unconformably tuffs (t) and sandstones (S); b) A view of the quaternary alluviums (Q^{al}) was deposited on the Eocene sandstones (ES). Layers of Q^{al} are horizontal; c) Layers of sandstone found in the toe slope during the cutting for the construction of bridge foundation. The figure clearly shows the high dip of the sandstone (65°).

The compositions of the fragments are tuff, andesite, and tuffite. In addition, excavation of the berms on April 2013 revealed young and old conglomeratic alluvial (Q_t) and recent alluvial fans (Q_f) lying discontinuously on the bedrock. The alluvial conglomerate is covered by olive garden and trees (Figure 4b). Moreover, during the excavation of the road bridge foundation, sandstone with a dip/dip direction of 65°/130° was detected. Therefore, based on these explanations and the excavation observations, it can be stated that the

[Downloaded from ndea10.khu.ac.ir on 2026-11-03]

[DOR: 20.1001.1.22286837.1398.13.5.4.3]

freeway floor is located on the sandstone (Figure 4c). Geological setting and section are presented in Figures 6 and 7, respectively [16] and [17].

Site investigations and field data

Site investigations have been done in January 15, 2015, enable us to describe the depth and the shape of the slide as well as striations on the slip surface. For this **purpose**, two test pits (P_1 and P_2) and boreholes were excavated (Figu**r**e 1). Test pits and test trenches permit a direct inspection of the individual rock strata and easy extraction of undisturbed samples for laboratory research [18]. Test trench was excavated near the D_2 and P_1 was excavated near the D_3 compared to P_2. The shape and striations on the slip surface from the test trench are shown in Figure 5a. As can be seen clearly in Figure 5b and 5c, the slip surface has a curved shape at the toe of the landslide and passes below D_2 with a dip angle of 10˚. A dip direction of striations on the slip surface was 240˚ (Figure 5b). The surveys also demonstrated that the slip surfaces were formed near the boundary of the volcanic breccias (VB) and tuffs (t) from the Karaj formation, resulting in the sliding of the tuffs (Figure 5c). In this excavation, up to a depth of 5 m of freeway bed, the material is red marls with tuff. The sliding surface in the P_1 appeared on January 30, 2015, but in the P_2 it was not observed since it was in at rest state. The opening of crack is perpendicular to the freeway and has a 210˚ direction. According to Chowdhury et al. (2013) [18], if the thickness of moving layer does not exceed 1.5 m, the slide is described as a surface landslide, less than 5 m, as shallow; from 5 to 20 m, as deep;

[Downloaded from ndea10.khu.ac.ir on 2026-11-03]

[DOR: 20.1001.1.22286837.1398.13.5.4.3]

and more than 20 m it is called as very deep. The depth of a slide is usually measured at right angles to the surface of the slide. On the basis of this classification, the sliding surface in the Manjil landslide is deep stated. As mentioned earlier, 9 boreholes were drilled in the toe slope and the floor freeway. The results of boreholes are shown in Table 1.

Methods

Analysis of the stability Manjil landslide with PHASE^{2D} program includes the following steps:

1- Determination of the critical safety factor, slip surfaces at the different parts of the slope by shear strength reduction based on finite element method (SSR-FEM) and site investigation.

Table 1. Characteristics of boreholes drilled at the toe slope of Manjil landslide.

Borehole	Drilled borehole location in km of the Freeway	Drilling depth (m)	Boundary between rock and soils (m)
BH1	42+137	20	Not specified
BH2	42+200	17	14
BH3	42+000	18	12
BH4	42+068	13	10
BH1-1	42+010	20	10
BH2-1	42+040	21	12
BH3-1	42+065	Because of mudslides, drilled to a depth of 5.7 m	
BH3-2	42+063	Because of mudslides, drilled to a depth of 7 m	
BH4-1	42+100	20	16

Determination and presentation of the methods to improve the slope stability.

In order to determine an optimal method, a factor of safety (FS), the maximum bending moment, the maximum shear force and the maximum shear displacement in the static and pseudo-static states are computed.

Moreover, in this study, using the deterministic approach, Peak

[Downloaded from ndea10.khu.ac.ir on 2026-11-03]

[DOR: 20.1001.1.22286837.1398.13.5.4.3]

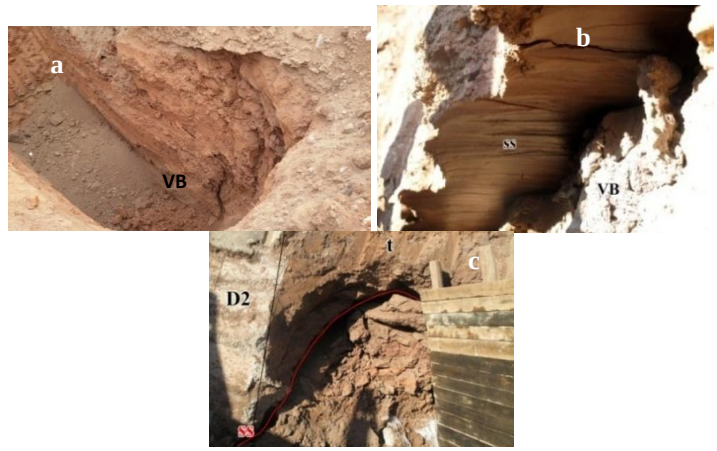


Figure 5. a) the slip surface appeared in the P1 (January 30, 2015) (view toward the northwest); b) striations **on the slip surface (ss) below D2 (January 15, 2015) (view toward the southwest) and c) A view of the slip surface curve where the toe of the landslide passes below D2.**

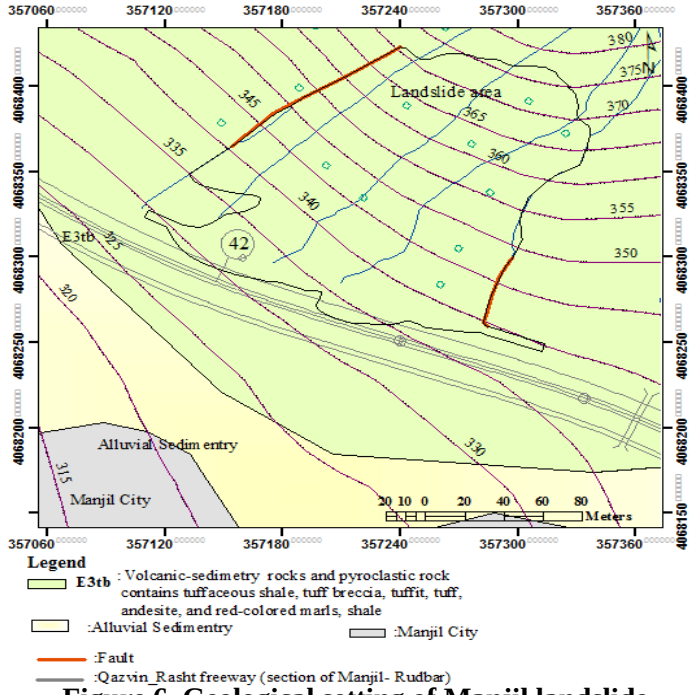


Figure 6. Geological setting of Manjil landslide.

[Downloaded from ndea10.khu.ac.ir on 2026-11-03]

[DOR: 20.1001.1.22286837.1398.13.5.4.3]

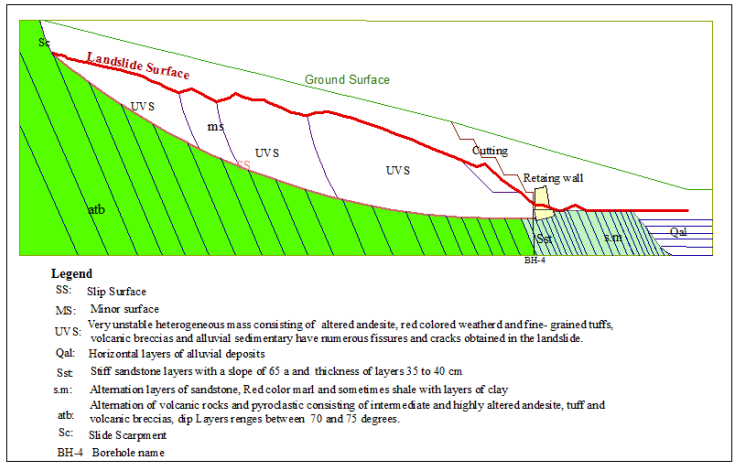


Figure 7. Geological section of Manjil landslide.

Ground Acceleration (PGA) in a radius of 200 km of Manjil landslide is considered to calculate the slope stability in the pseudo-static state.

Seismic Hazard Assessment

In an earthquake ground motion hazard evaluation, determination of peak ground motion (PGA) of the slope is an important issue. Two approaches, probabilistic seismic hazard analysis (PSHA) and deterministic seismic hazard analysis (DSHA), are commonly used for seismic hazard assessment. In this study, seismic hazard assessment using the deterministic approach in a radius of 200 km of Manjil landslide is carried out. Seismic source zones with complete earthquake's catalogue and faults in a radius of 200 km are shown in Figure 8. As can be seen in this figure, a number of the main and potential earthquake faults are detected such as Rudbar, Manjil, Harzevil, Khazar, Taleghan, Talesh, Lahijan, Masuleh, Eshtehard, Ipak and Avaj and North Qazvin faults and etc. Different earthquakes

[Downloaded from ndea10.khu.ac.ir on 2026-11-03]

[DOR: 20.1001.1.22286837.1398.13.5.4.3]

(historical and instrument) were recorded in the studied area. For example, Manjil-Rudbar earthquake occurred at 0:30 A.M. (local time) on 20 June 1990 the northern part of Iran. According to the report of USGS, the magnitude of this earthquake was 7.6 on Richter scale (Ms=7.6, Mb=6.8) and the epicenter was South-West of Caspian Sea, latitude 36.96 N and longitude 49.41 E, with a focal depth about 10 km. Qazvin earthquake was occurred on 10 December 1119 in Qazvin with a magnitude of Ms=7.6. Earthquakes of 874 in Gonbade Kabus with magnitude Ms=6, earthquake of 1383 in Kojur -Firuzabad (Baladeh) with a magnitude of Mw=6.3, are attributed to the Khazar fault. Earthquakes such as of 1428, 20 April 1608, and 16 December 1808, were probably related to the Taleqan fault [19], [20] and [21]. Earthquake occurred at 18:57 P.M. (local time) on 5 December 2017 in Langroud cityat the intersection of the north Alborz and Lahijan faults. Maximum Magnitude (M_w) potential for different faults and historical and instrument earthquakes for each seismic source zones based on relationships of [20], [23] and [24] are presented in Table 2.

Final M_w for each seismic source zones are calculate using a logical tree as shown in Figure 9 and are present in Table 3. Attenuation relation derived by Boore et al. (1997) [25] are used for calculation the PGA_{max} which is based on data from western north America for the magnitude range 5-7.7 and a distance less than 100 km. The attenuation relation is as follows:

$$\text{Log PGA}= b_1+b_2\,(M-6)+b_3\,(M-6)^2+b4\sqrt{R^2+h^2}+b_5\log\left(\sqrt{R^2+h^2}\right)+b_6G_B+b_7G_C \quad (1)$$

[Downloaded from ndea10.khu.ac.ir on 2026-11-03]

[DOR: 20.1001.1.22286837.1398.13.5.4.3]

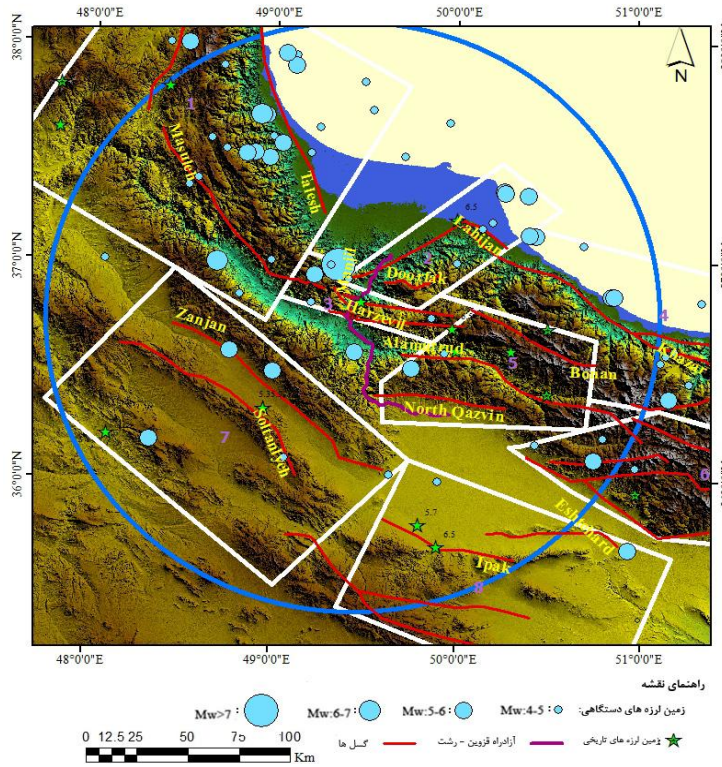


Figure 8. Aerial image with seismic source zones, historic and instrument earthquake, and faults in the 200 km radius of the Manjil landslide. The red lines represent faults. The gray lines define the seismic source zones and green stars and black points represent the historic and instrument earthquake, respectively. Moreover, Qazvin-Rasht freeway and Manjil landslide are shown in violet line and red point, respectively.

Where, PGA is a peak ground acceleration (g), M is Magnitude, R is minimum distance from the study area to the fault, G_B and G_C are soil type factors. Results of PGA_{max} and R_{min} are presented in Table 3. As can be seen in the table, the value of 0.45 is obtained for PGA_{max}, which is related to the source 3. It seems that the reason is due to the proximity of the Manjil landslide to the active faults of Manjil and Rudbar.

[Downloaded from ndea10.khu.ac.ir on 2026-11-03]

[DOR: 20.1001.1.22286837.1398.13.5.4.3]

Table 2. Results of maximum magnitude (M_w) potential for different faults in the study area based on relationships of Zare (1995), Mohajer ashjaii- Noruzi (1984), Wells and Coppersmith (1994)

Seismic source zones	Fault	Length of fault	Zare (1995)		Mohajer ashjaii-Noruzi (1984)		Wells and Coppersmith (1994)		Instrument record	Historic record
			Mw=0.91lnLR+3.66		M=log L+5.4		M=5.08+logL			
			LR=0.37LF	Mw	L=0.5LF	Ms	L=0.5LF	Mw		
1	Talesh	488	180.56	8.39	244	244	244	7.85	6.45	6.9
	Sangavar	55	20.35	6.4	27.5	27.5	27.5	6.51		
	Masuleh	62	22.94	6.51	31	31	31	6.8		
2	Lahijan	53	19.61	6.37	26.5	26.5	26.5	6.73	5.6	6.5
3	Rudbar	80	29.6	6.74	40	40	40	6.93	7.6	7
	Manjil	65	22.2	6.48	32.5	32.5	32.5	6.83		
	Harzevil	5.5	2.035	4.3	2.75	2.75	2.75	5.59		
	Taklim	62	22.94	6.51	31	31	31	6.8		
	Ali Abad	8.5	3.145	4.7	4.25	4.25	4.25	6.02		
4	Khazar	600	229.4	8.6	300	300	300	7.96	5.28	6.8
	North Alborz	310	114.7	7.97	155	155	155	7.62		
5	Bonan	67.5	24.975	6.58	33.75	33.75	33.75	6.67	7.2	7.6
	Alamutrud	110	40.7	7.03	55	55	55	7.09		
	North Qazvin	65	24.05	6.55	32.5	32.5	32.5	6.83		
6	Taleghan	67	24.79	6.58	33.5	33.5	33.5	6.84	7.6	7.1
	North Tehran	108	39.96	7.01	54	54	54	7.1		
7	Soltaniey	140	51.8	7.25	70	70	70	7.22	5.4	6.1
	Zanjan	72	26.64	6.64	36	36	36	6.88		
8	Eshtehard	100	37	6.94	50	50	50	7.05	7.2	6.5
	Ipak	85	31.45	6.8	42.5	42.5	42.58	6.96		
	Avaj	60	22.2	6.48	30	30	30	6.79		

LR: surface rapture length in km. LF: Length of fault

[Downloaded from ndea10.khu.ac.ir on 2026-11-03]

[DOR: 20.1001.1.22286837.1398.13.5.4.3]

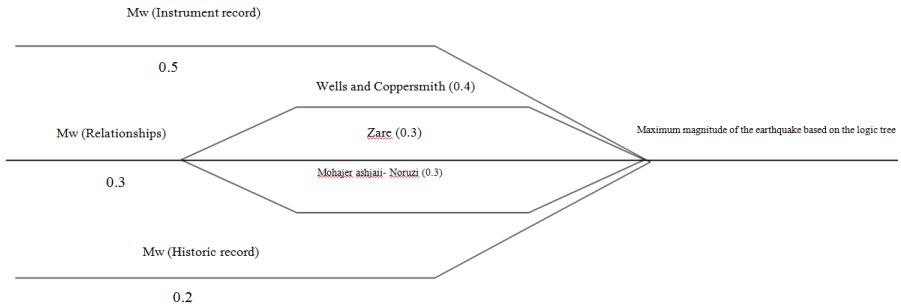


Figure 9. Logical tree are used for M_w

Table 3. M_w and PGA_{max} for each seismic source zones in the 200 km radius of the Manjil landslide

Source	1	2	3	4	5	6	7	8
M_w	7	6.1	7.26	6.45	7.24	7.19	6.1	7
R_{min} (Km)	36.4	16	0.5	45.8	42.5	99.8	77.5	37.5
PGA_{max} (g)	0.09	0.1	0.45	0.06	0.1	0.05	0.03	0.09

Landslide modeling using the continuum analysis in PHASE^{2D}

To propose a stabilization program for Manjil landslide, it was simulated using the continuum analysis in PHASE^{2D}. Two-dimensional 3-noded triangular plane strain elements were used to discretize across selected slope profile for a landslide. PHASE^{2D} automatically computes the ground surface above the element and automatically determines the stress due to the material above the element. The horizontal to vertical stress ratio ($\frac{\delta_h}{\delta_v}$) is kept as 1.0 [26]. The body force is calculated using the unit weight defined for the material. Fixed boundary conditions were assumed along the lateral side and base of the model such that the displacement which is restrained in both x and y directions. The slope face was kept free. The boundary conditions of the model and the FEM mesh of Manjil

[Downloaded from ndea10.khu.ac.ir on 2026-11-03]

[DOR: 20.1001.1.22286837.1398.13.5.4.3]

landslide are displayed in Figure 10. In areas with sliding mass probability, the choice of a suitable distance requires accurate analysis while in area far from sliding mass it is not of great importance. Therefore long distances are considered for meshing. Mohr-Coulomb failure criterion is used for soil, while piles are taken as linear elastic materials. One of the major features of PHASE^{2D} is the model of the piles using structural elements considering pile/soil interaction.

1. Overview of the SSR method

In the analysis of slope stability, it is important to obtain the safety factor and slip surface There are several ways to calculate the safety factor. One of the methods used in the most of numerical software to calculate this parameter is the shear strength reduction method (SSR). Moreover, one of the advantages of the SSR method is that there is no need to guess at determination of critical failure surface.

In the SSR-FEM, the reduced shear strength parameters c_R and φ_R are given as follows:

$$c_R = \frac{c}{F} \tag{2}$$

$$\varphi_R = tan^{-1}\left(\frac{tan\varphi}{F}\right) \tag{3}$$

Where, F is a strength reduction factor, and c and φ are the original shear strength parameters.

In order to obtain a reliable factor of safety, the strength reduction factor (F) needs to be gradually increased until the reduced strength parameters (c_R and φ_R) bring the slope into the failure state. At this time, the safety factor for the slope is equal to the strength reduction factor, i.e., FS=F [27].

[Downloaded from ndea10.khu.ac.ir on 2026-11-03]

[DOR: 20.1001.1.22286837.1398.13.5.4.3]

After construction of the slope's geometry and cutting process using excavation berms with a width and height of 4 m and 6 m, respectively and a 5 to 6 m excavation depth within a 120 m line along the slope toe (Figure 7), the steps for systematic searchof the critical factor of safety value F that brings a previously stable slope ($F \geq 1$) to the verge of failure are as follows: Step 1: Development of a FE model for the slope, using the appropriate material deformation and strength properties. Compute the model and record the maximum total deformation. Step 2: Increasing the F value (or strength reduction factor) and calculating Mohr-Coulomb parameters as described above. Entering the new strength properties into the slope model and re-computing and recording the maximum total deformation. Step 3: Repeating Step 2, using systematic increments of F, until the FE model does not converge to a solution, i.e. continue to reducing material strength until the slope fails. The critical F value at which failure occurs is the factor of safety. For a slope with a factor of safety less than 1, the procedure remains the same except for use of systematically reduced F values (this is equivalent to increasing the shear strength parameters of materials) until the slope becomes stable. Due to the use of factored strength parameters as input into models, the SSR technique can be used with any existing FE software. The only task required to analyze the slope is computation of Mohr-Coulomb strength parameters as input values for FE model. Phase^{2D} is a powerful and flexible computer package that has the Shear Strength Reduction (SSR) method integrated into the FEM and interpretation modules. Geotechnical parameters

[Downloaded from ndea10.khu.ac.ir on 2026-11-03]

[DOR: 20.1001.1.22286837.1398.13.5.4.3]

obtained are represented in Table 4. Contours of maximum shear strain and critical safety factor by SSR method for Manjil landslide are shown in Figure 11. As can be seen in Figure, the critical SRF is found to be 0.98 and higher concentration of shear strain along the toe region and the stability will get reduced and may initiate failure. Moreover, the depth and angle of the critical slip surface at different parts of the slope are indicated by contours of maximum shear strain. In the section, in addition to the SSR method, the trenches and pits test (P1 and P2) and boreholes drilled in the toe landslide (Table 1) and the observations described in Section 2 have been used and compared. The FE analysis results indicated the instability of the slope below road level along a particular plane (slip surface). This is also validated with the actual sliding below road level as shown in the field photograph (Figure 5a, b and c).

Table 4. Geotechnical parameters adopted for stability analysis

Material	Model	Unit weight γ (kN/m^3)	Shear strength		Elastic modulus (MPa)	Poisson's ratio
			c (kPa)	φ (˚)		
Sliding mass	Mohr-Coulomb	20	20	18	20	0.35
Sandstone	Mohr-Coulomb	22	50	35	70	0.30
Bed rock	Mohr-Coulomb	25	200	36	200	0.25

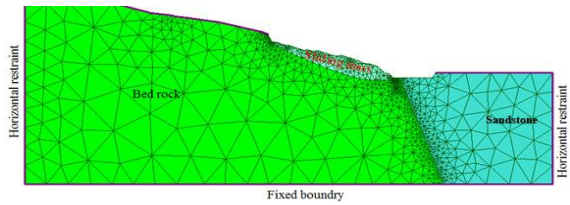


Figure 10. Finite element mesh and boundary conditions used in the numerical analysis

[Downloaded from ndea10.khu.ac.ir on 2026-11-03]

[DOR: 20.1001.1.22286837.1398.13.5.4.3]

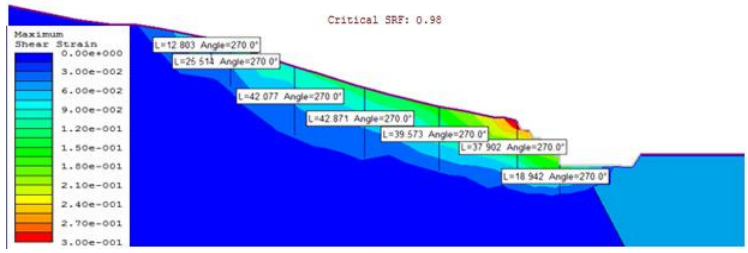


Figure 11. The depth and angle of the critical slip surface at different parts of the slope indicated by contours of maximum shear strain

The model analysis of Manjil landslide continued with light weighting and flattening of the slope to reach a balance for the potential sliding mass at the static condition. In the first stage, the red marls and alluvial sediments which are extended beneath the freeway floor, were excavated. The estimated amount of excavated sliding mass is approximately 130,000 m^3. Then, the surface of sliding mass was flattened at an angle of 19˚-25˚, i.e. loose dangerous blocks on the slopes were removed, which has been illustrated by nodes and elements drawn above the sliding mass in Figures 12 and 16. Finally, stabilization method applied in a landslide is the piling and insufficient retaining walls based on the slip surface in Manjil landslide (site investigation section and Figure 11) are performed. Computing the model and recording the maximum bending moments, shear forces and shear displacements of the structural elements in the static and pseudo-static states were obtained. A pseudo-static approach was mostly used in seismic slope stability analysis, where the effects of an earthquake are represented by constant vertical and/or horizontal accelerations [28]. Hynes-Griffin and Franklin (1984) [29] suggested that appropriate pseudo-static

[Downloaded from ndea10.khu.ac.ir on 2026-11-03]

[DOR: 20.1001.1.22286837.1398.13.5.4.3]

coefficients for earth slopes should be one-half of the peak ground acceleration. For this reason, a maximum of 225 cm/s^2 horizontal seismic acceleration (one-half of 450 cm/s^2) was taken into consideration in the Manjil landslide (Figure 8 and Table 3).

Slope Stabilization Methods

1. Single pile (SP)

As mentioned above, the piles are modeled using structural elements with pile/soil interface, and the properties of the interface do not significantly affect the model results because of the soft nature of the surrounding soil. The parameters of the concrete piles and backfill used for the finite element analysis are presented in Table 3.

Safety factors for the final stabilization slope with a single pile in the static and pseudo-static analysis are shown in Figures 13a and

Table 5. Parameters of concrete pile and backfill are used at the SP for the finite element analysis.

Type of structure	Model	Parameter	Value
Concrete Pile	Linear elastic	Linear Type	Reinforced concrete
		Length (m)	25
		Section depth(m)	1.8
		Young's modulus (MPa)	20,000
		Poisson's ratio	0.2
		Unit Weight (MN/m^3)	0.025
		Compressive strength (MPa)	25
		Tensile strength (MPa)	2.5
		Area (m^2)	2.54
		Moment of inertia (m^4)	0.52
Backfill	Mohr-Coulomb	Young's modulus (MPa)	50
		Poisson's ratio	0.3
		Unit Weight (MN/m^3)	0.022
		Cohesion (MPa)	0
		Friction angle (°)	35

13b, respectively. The bending moment and shear force on piles are two key factors to evaluate the stabilization. The maximum shear force, maximum shear displacement and maximum bending moment

[Downloaded from ndea10.khu.ac.ir on 2026-11-03]

[DOR: 20.1001.1.22286837.1398.13.5.4.3]

of single pile in the static and pseudo-static analyses are shown in Figures 14 and 15, respectively. As illustrated in Figure 13.b, calculated FS for the static analysis is 1.95 while it is 1.17 for pseudo-static state considering a seismic acceleration of 225 cm/s^2. The calculated FS is acceptable even in pseudo-static conditions, considering degree of risk in the landslide area.

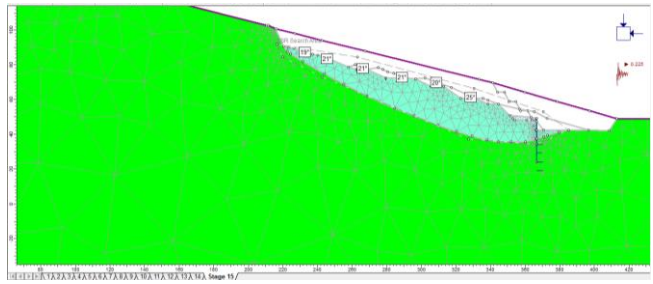


Figure 12. Stabilization of Manjil landslide with SP for the pseudo-static analysis

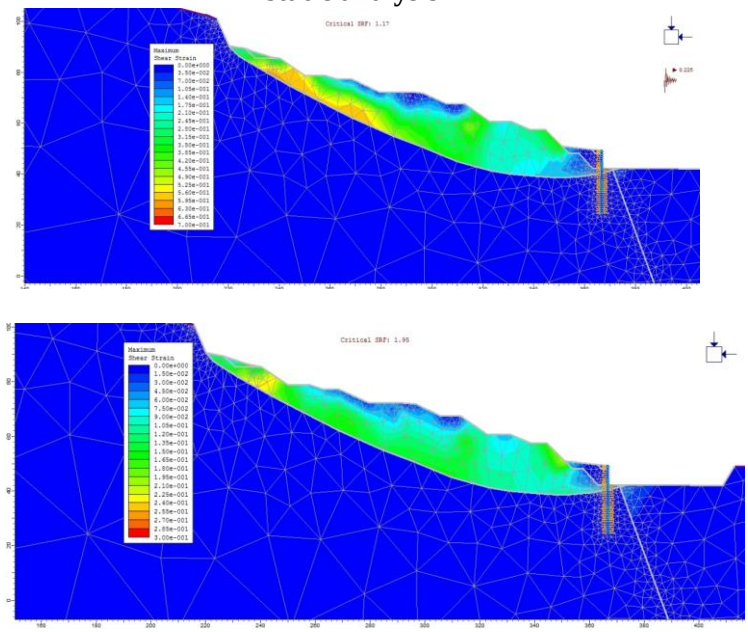


Figure 13. Safety factor, nodal displacement increments and critical

[Downloaded from ndea10.khu.ac.ir on 2026-11-03]

[DOR: 20.1001.1.22286837.1398.13.5.4.3]

slip induced by shear strength reduction method with SP: a) Static analysis and b) Pseudo-static analysis.

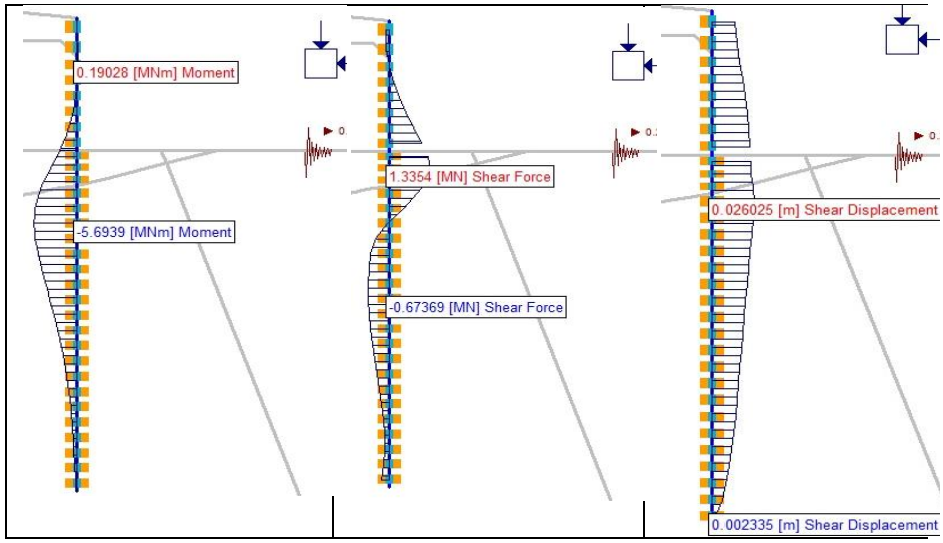


Figure 14. Pile behavior for SP in the pseudo-static analysis: a) Pile bending moment, b) Pile shear force, and c) Pile shear displacement.

2. Pile-to-pile cap connections (two pile group: 2PG)

Pile cap is defined as a concrete block cast on the head of a pile, or a group of piles, to transmit the load from the structure to the pile or group of piles. The individual piles are spaced and connected to the pile cap. The pile cap distributes the applied load to the individual piles which, in turn, transfer the load to the bearing ground. External pressures on a pile are likely to be greatest near the ground surface. Ground stability increases with depth and pressure. The top of the pile therefore, is more vulnerable to movement and stress than its base. Pile caps are thus incorporated in order to tie the pile heads together so that individual pile movement and settlement are greatly

[Downloaded from ndea10.khu.ac.ir on 2026-11-03]

[DOR: 20.1001.1.22286837.1398.13.5.4.3]

reduced. Thus stability of the pile group is greatly increased. The functions of a pile cap are:

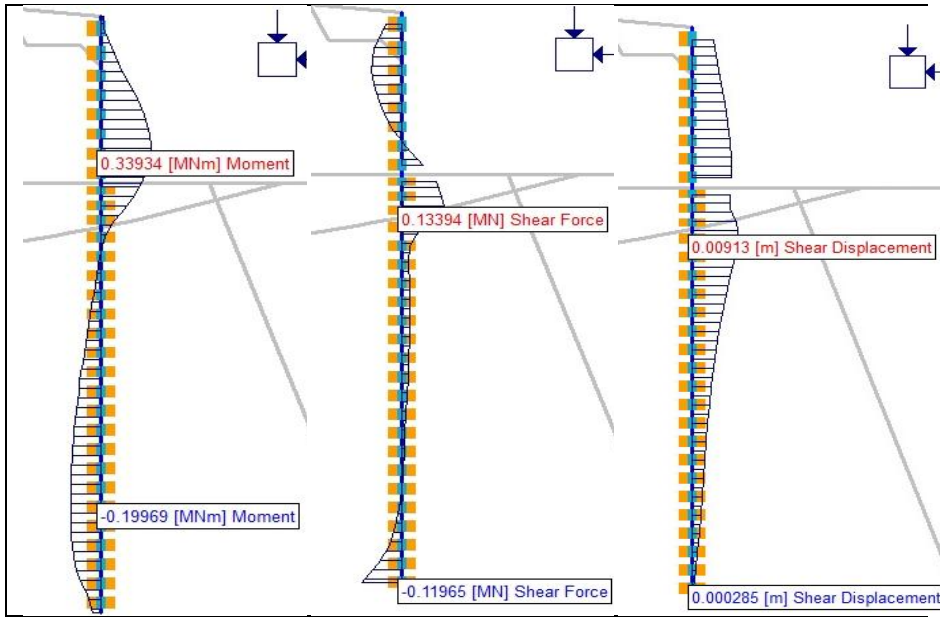


Figure 15. Pile behavior for SP in the static analysis: a) Pile bending moment, b) Pile shear force, and c) Pile shear displacement.

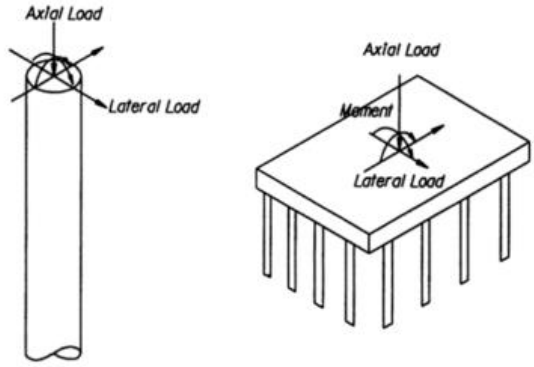


Figure 16. Acting loads on top of a pile or a pile group: a) Single pile and b) Pile group [30].

[Downloaded from ndea10.khu.ac.ir on 2026-11-03]

[DOR: 20.1001.1.22286837.1398.13.5.4.3]

1. To distribute a single load equally over the pile group and thus over a greater area of bearing potential.
2. To laterally stabilize individual piles and thus increasing overall stability of the group.
3. To provide the necessary combined resistance to stresses set up by the super structure and/or ground movement [30]. Figure 15 illustrates acting loads on the top of a pile group in addition to those of individual piles.

Due to the high bending moment on the pile (Figure 14), cost reduction and sustainable functionality, double pile-to-pile cap connections were designed at the toe of the slope. In this work, the excavation of sliding mass, flattening of the slope, backfill properties and length of piles were kept constant. Other characteristics of the piles and pile cap used for the 2PG in the Manjil landslide are presented in Table 6.

Table 6. Parameters of the concrete pile and pile cap are used for the 2PG for the finite element analysis.

Type of structure	Model	Parameter	Value
Concrete pile	Linear elastic	Diameter (m)	1.2
		Length (m)	25
		Depth section (m)	1.2
		Distance between two pile group (m)	3.6
		Area (m^2)	2.54
pile cap	Linear elastic	Width (m)	1.5
		Moment of inertia (m^4)	0.102
		Young's modulus (MPa)	20,000
		Poisson's ratio	0.2

The simulated models for the 2PG in the pseudo-static analysis are shown in Figure 17 and FS values in the static and pseudo-static analysis are presented in Figure 18a and 18b, respectively. As

[Downloaded from ndea10.khu.ac.ir on 2026-11-03]

[DOR: 20.1001.1.22286837.1398.13.5.4.3]

illustrated in Figure 18.b, FS calculated for the static analysis is 1.95 while it is 1.17 for pseudo-static state considering a 225 cm/s^2. The effect of 2PG on the pile behavior (maximum bending moment, shear force and shear displacement) for both analyses are calculated and displayed in Figures 19 and 20. As demonstrated in Figure 20, for 2PG system, the maximum bending moment of piles decreases from 5.69 to 2.48 MN/m, which is almost halved.

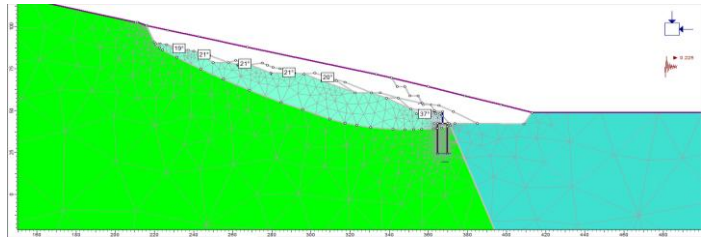


Figure 17. Stabilization of Manjil landslide with 2PG in the pseudo-static analysis.

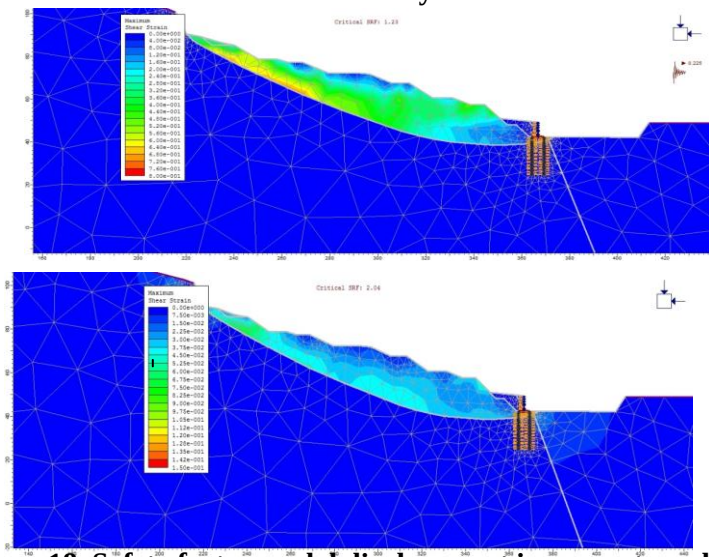


Figure 18. Safety factor, nodal displacement increments and critical slip induced with shear strength reduction method using 2PG: a) Static analysis and b) Pseudo-static analysis

[Downloaded from ndea10.khu.ac.ir on 2026-11-03]

[DOR: 20.1001.1.22286837.1398.13.5.4.3]

Discussion

Manjil landslide in Alborz mountainous is located at 41+400 km to 42+200 km along the Qazvin-Rasht freeway, was occurred due to inappropriate cutting in June 2013 and led to closure of freeway. The deterministic seismic hazard assessment (DSHA) study was carried out in the 200 km radius of the Manjil landslide. It can be concluded that Manjil landslide has a PGA value of 45cm/s^2 (Figure 8).

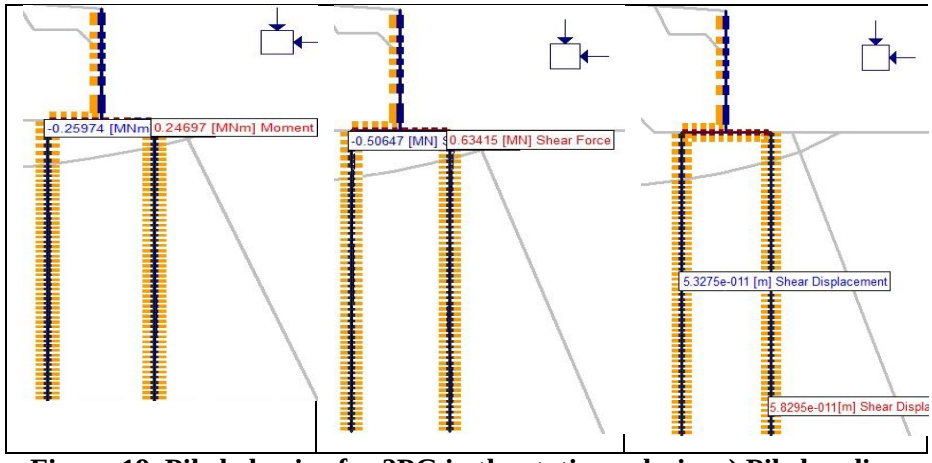


Figure 19. Pile behavior for 2PG in the static analysis: a) Pile bending moment, b) Pile shear force, and c) Pile shear displacement.

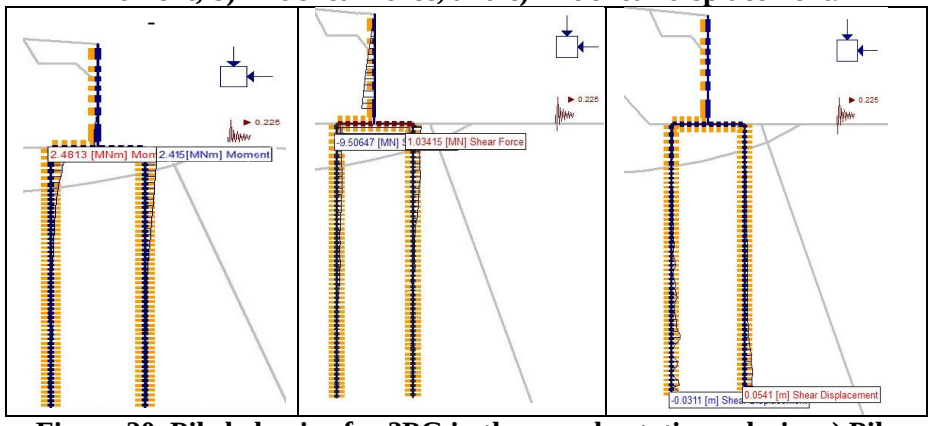


Figure 20. Pile behavior for 2PG in the pseudo-static analysis: a) Pile bending moment, b) Pile shear force, and c) Pile shear displacement.

[Downloaded from ndea10.khu.ac.ir on 2026-11-03]

[DOR: 20.1001.1.22286837.1398.13.5.4.3]

In this study, depth and angle of the critical slip surface was determined by SSR method. The FE analysis result indicated the instability of the slope below road level along a particular plane (slip surface). This was also validated with the actual sliding below road level (observation of trenches, pit tests and boreholes drilled in the toe landslide) as shown in the field photograph (Table 1 and Figures 5a, 5b and 5c). After determination of critical slip surface, for stabilization of Manjil (Figure 11) light weighting and flattening of sliding mass and length of piles were kept constant. Then for stabilization Manjil landslide,SP and 2PG systems were evaluated by static and pseudo-static analyses. As mentioned above, appropriate pseudo-static coefficients for earth slopes should be one-half of the peak ground acceleration. For this reason, a maximum of 225 cm/s^2 horizontal seismic acceleration (one-half of 450 cm/s^2) are taken into consideration in the Manjil landslide. The parameters of the piles are extracted from the FE analysis results so that the slip surface is located below road level. For stabilization of landslide, the height of the pile from the bottom of the freeway is 18 meters (Figure 12) and the total height of 25 meters should be considered. The diameter, area of the piles and distance between two pile groups are about 1.2 m and 2.54m^2 and 3.6 m, respectively.

As displayed in Figure 14, the pile maximum bending moment around the slide surface is significantly high (5.69 MN.m) more than the bending moment capacity of a pile. Therefore, the pile fails due to bending. Also, dispersion of the shear force and displacement in the pile and the wall has been added. Due to the high bending

[Downloaded from ndea10.khu.ac.ir on 2026-11-03]

[DOR: 20.1001.1.22286837.1398.13.5.4.3]

moment on the pile (Figure 14), cost reduction and sustainable functionality, double pile-to-pile cap connections are considered at the toe of the slope. One of the important tasks pile cap is distribution of forces between them. Duan et al., (2014) [30] stated that a pile group is more efficient in resisting overturning and moment than an individual foundation. For a pile group, through the action of the pile cap, the coupled axial compressive and uplift resistance of individual piles provides the majority of resistance to the overturning moment loading. The results of numerical analysis are shown in Figures 19 and 20. The comparison results between SP and 2PG are given in Table 5. The results indicate that the safety factor (FS) in the pseudo-static analysis increases from 1.95 to 2.04. For a 2PG, through the action of the pile cap, maximum bending moments are improved compared to SP which decreased from 5.29 to 2.48 MN/m, which is almost halved. Shear force are 9.5 MN for Pile 1 and 1 MN for Pile 2. Therefore, the equal shear force can be seen at the top of the piles. It can be concluded that the pile cap has well distributed forces between the piles and did not collapse because of a shear failure.

On the other hand, by checking changes in the amount of displacement at the piles in the SP and 2PG stabilized slopes, it is found that the amount of displacement in the two-pile piles decreased. The displacement of the end of the pile in the static and the pseudo-static state is 5.32×10^{-11} and 0.05 m, respectively. Moreover, the end of the pile is installed in to a bedrock stratum. It has been stated that the piles should be installed into a stable stratum

[Downloaded from ndea10.khu.ac.ir on 2026-11-03]

[DOR: 20.1001.1.22286837.1398.13.5.4.3]

to improve the stability of slopes and prevent potential landslides [31-35].

Table 5. Comparison of the obtained results between slope stabilization methods slopes with single pile and two pile groups

Parameters obtained	Single pile		Two pile groups	
	Static analysis	Pseudo-static analysis	Static analysis	Pseudo-static analysis
Maximum bending moment (MN.m)	0.33	5.69	0.26	2.48
Maximum Shear force (MN.m)	0.13	1.33	0.63	1.004
Maximum displacement at the top of the pile (m)	0.009	0.026	0	0
Maximum displacement at the end of the pile	0.0003	0.0023	5.32×10^{-11}	0.054
Maximum displacement at the pile cap	-	-	0	0
Safety factor	1.95	1.17	2.04	1.23

Conclusions

In Manjil landslide stabilization it can be concluded that after light weighting and flattening of sliding mass and system balance, the pile-to-pile cap connections (Two pile groups- 2PG) showed the optimum performance. The safety factor (FS) in the pseudo-static state increased from 1.95 to 2.04. Moreover, maximum bending moments improved compared to SP which decreased from 5.69 to 2.48 MN/m, which is almost halved. For a 2PG, the maximum shear force and shear displacement decreased for two piles.

[Downloaded from ndea10.khu.ac.ir on 2026-11-03]

[DOR: 20.1001.1.22286837.1398.13.5.4.3]

References

1. Barla G., Antolini F., Barla M., "Slope stabilization in difficult conditions: the case study of a debris slide in NW Italian Alps", Landslides. 10(2013) 343-355.
2. Fellenius W., "Calculation of the stability of earth dams", Transactions of the 2nd congress on large dams, Washington, DC. 4(1936) 445-463.
3. Janbu N., "Application of composite slip surfaces for stability analysis", Proceedings of the European conference on stability of earth slopes, Stockholm. 3 (1954) 43-49.
4. Bishop A., "The use of the slip circle in the stability analysis of earth slopes", Gotechnique. (1) 5 (1955) 7-17.
5. Morgenstern N., Price V. E., "The analysis of the stability of general slip surfaces", Geotechnique. (1) 15(1965) 79-93.
6. Spencer E. A., "Method of analysis of the stability of embankments assuming parallel inter-slice forces", Geotechnique. (1)17(1967) 11-26.
7. Chakraborti S., Konietzky H., Katrin W.A., "Comparative study of different approaches for factor of safety calculations by shear strength reduction technique for non-linear Hoek-Brown failure criterion", Geotech Geol Eng. 30 (2012) 925-934.
8. Kanungo D. P., Pain A., Sharma Sh., "Finite element modeling approach to assess the stability of debris and rock slopes: a case study from the Indian Himalayas", Nat Hazards. 69 (2013) 1-24.
9. Budetta P., "Stability of an undercut sea-cliff along a Cilento coastal stretch (Campania, Southern Italy)", Nat Hazards. 56 (2011) 233-250.
10. Usluogullari O.F., Temugan A., Duman E.S., "Comparison of slope stabilization methods by three dimensional finite element analysis", Nat Hazards. (2) 81 (2016) 1027-1050.

[Downloaded from ndea10.khu.ac.ir on 2026-11-03]

[DOR: 20.1001.1.22286837.1398.13.5.4.3]

11. Chen X. P., Zhu H. H., Huang J. W., Liu D., "Stability analysis of an ancient landslide considering shear strength reduction behavior of slip zone soil. Landslides", (1) 13 (2016) 173-181.
12. Cai F., Ugai K., "Numerical analysis of the stability of a slope reinforced with piles. Soils and foundations", (1) 40 (2000) 73-84.
13. Ashour M., Ardalan H., "Analysis of pile stabilized slopes based on soil-pile interaction", Computers and Geotechnics. 39 (2012) 85-97.
14. Rocscience A., "2D finite element program for calculating stresses and estimating support around the underground excavations", Geomechanics software and research, Rocscience INC, Toronto, Canada. (2012).
15. Can E., "Investigation of landslide potential parameters on Zonguldak-Ereğli highway and adverse effects of landslides in the region", Environ Monit Assess.186. (2014) 2435-2447.
16. Geological Survey of Iran. "1:25,000 Geology map of Rudbar (Khalil Abad)", Geological Survey of Tehran, Iran (2016).
17. Ghobadi M. H., Firuzi M., Noorzad A.,"A large-scale landslide and related mechanism: a case study in the Qazvin-Rasht freeway, Iran". Environmental Earth Sciences, (14) 76 (2017) 478.
18. Chowdhury R., Flentje P., Bhattacharya G., "Geotechnics in the Twenty-First Century, Uncertainties and Other Challenges: With Particular Reference to Landslide Hazard and Risk Assessment." In Proceedings of the International Symposium on Engineering under Uncertainty: Safety Assessment and Management. (2013) 27-53.
19. Berberian M., "Contribution to the seismotectonics of Iran (part II-III): In commemoration of the 50th anniversary of the Pahlavi dynasty", Ministry of Industry and Mines, Geological Survey of Iran, Tectonic and Seismotectonic Section. 30 (1976).

[Downloaded from ndea10.khu.ac.ir on 2026-11-03]

[DOR: 20.1001.1.22286837.1398.13.5.4.3]

20. Ambraseys N. N., Melville C. P. "A History of Persian Earthquakes", Cambridge University Press, Cambridge, UK. (1982).
21. http://www.iiees.ac.ir.
22. Zare M., "Site sependent attenuation of strong motions for Iran", Proceedings of the Fifth International Conference on Seismic Zonation, Nice, France (1995) 1227-1236.
23. Mohajer-Ashjai A., Noroozi A. A., "Observed and probable intensity zoning of Iran",.Tectonophysics.49 (1978) 149-160.
24. Wells D. L., Coppersmith K. J., "New empirical relationships among magnitude, rupture length, rupture width, rupture area, and surface displacement", Bulletin of the seismological Society of America. 84 (4) (1994) 974-1002.
25. Boore D. M., Joyner W. B., Fumal T. E.,"Equations for estimating horizontal response spectra and peak acceleration from western North American earthquakes: A summary of recent work", Seismological research letters 68(1) (1997) 128-153.
26. Pal S., Kaynia A. M, Bhasin R. K., Paul D. K., "Earthquake stability analysis of rock slopes: a case study", Rock Mech Rock Eng. 45 (2012) 205-215.
27. Wang J. J., Liang Y., Zhang H. P., Wu Y., Xin L., "A loess landslide induced by excavation and rainfall", Landslides. 11 (2014) 141-152.
28. Kramer S. L., "Geotechnical earthquake engineering", Prentice Hall, New Jersey (1996).
29. Hynes-Griffin M. E., Franklin A. G., "Rationalizing the seismic coefficient method", Miscellaneous Paper GL-84-13, U.S. Army Corps of Engineers Waterways Experiment Station, Vicksburg, Mississippi. (1984).

[Downloaded from ndea10.khu.ac.ir on 2026-11-03]

[DOR: 20.1001.1.22286837.1398.13.5.4.3]

30. Duan J., Chen,X. M., Qi H., Li Y. G., "An Integrated Simulation System for Building Structures", In Applied Mechanics and Materials, Trans Tech Publications. 580 (2014) 3127-3133.
31. Chen C., Martin G., "Soil-structure interaction for landslide stabilizing piles", Computers and Geotechnics. (5) 29 (2002) 363-386.
32. Lirer S., "Landslide stabilizing piles: experimental evidences and numerical interpretation", Eng Geol. 149 (2012) 70-77.
33. Song Y. S., Hong W. P., Woo K. S., "Behavior and analysis of stabilizing piles installed in a cut slope during heavy rainfall", Eng Geol. 129 (2012) 56-67.
34. Zhou C., Shao W., Westen C. J., "Comparing two methods to estimate lateral force acting on stabilizing piles for a landslide in the three Gorges Reservoir, China", Eng Geol. 173 (2014) 41-53.
35. Yu Y., Yq Shang., Hy Sun., Ez Wang., "Displacement evolution of a creeping landslide stabilized with piles", Nat Hazards. (2) 75 (2015) 1959-1976.

[Downloaded from ndea10.khu.ac.ir on 2026-11-03]

[DOR: 20.1001.1.22286837.1398.13.5.4.3]